

Intrinsic Fluorescence Study of the Interaction of Human Apolipoprotein H with Phospholipid Vesicles[†]

Shao-Xiong Wang, Guo-ping Cai, and Sen-fang Sui*

State-Key Laboratory of Biomembrane, Department of Biological Sciences & Biotechnology, Tsinghua University, Beijing 100084, People's Republic of China

Received January 13, 1999; Revised Manuscript Received April 7, 1999

ABSTRACT: Apolipoprotein H (ApoH) is a plasma glycoprotein with its in vivo physiological and pathogenic roles being closely related to its interaction with negatively charged membranes. In this paper, the interaction of ApoH with phospholipid vesicles was characterized by (i) detecting the wavelength shift of the fluorescence spectrum of ApoH and (ii) measuring the fluorescence quenching extent of ApoH by the membrane resident quencher 1-palmitoyl-2-stearoyl-(5-doxy)-sn-glycero-3-phosphocholine (DPC). The observed blue shift upon addition of DMPG vesicles indicated that the tryptophan residues of ApoH moved from a polar to a nonpolar environment. The insertion ability of ApoH into PG-containing vesicles did not depend on the PG content in a stoichiometric way as did the blue shift, indicating that the negatively charged DMPG does not serve as a specific binding site but rather provides a suitable microenvironment for ApoH interaction. The finding that the detachment effect of cations on the blue shift is remarkably different from that on the quenching extent suggests that ApoH is capable of existing in two different conformations when membrane-bound.

Apolipoprotein H (ApoH)¹ is a plasma glycoprotein either circulating as a free protein or associated to lipoproteins. This protein, also referred to as β_2 -glycoprotein I, was described for the first time in 1961 by Schultze et al. (1). Human ApoH is a single-chain molecule consisting of 326 amino acid residues and 5 carbohydrate chains, and has a molecular mass of approximately 54 kDa (2–5). The amino acid sequences of ApoH in human, bovine, mouse, and rat appear to be highly conserved (6–9). The protein contains 5 internal repeat units of 60 amino acid residues, each with 2 internal disulfide bonds, known as the Sushi domain (10). Since the solution structures of Sushi domains in three other proteins have been solved by the NMR method and been found to be very similar (11–13), it is feasible to create the structural model of ApoH by analogy.

Although quite a lot is known about the structure of ApoH, its biological function remains unclear. It is known that ApoH can bind to negatively charged substances such as DNA and heparin and negatively charged phospholipids etc. in vivo (14–16), but the meaning of such interaction is still unclear. Puurunen et al. compared ApoH with complement factor H, which also consists of Sushi domains, and found that these two proteins exhibited distinct function (17). It is now known

that ApoH may serve as a major factor in clearing the plasma liposome (18) as well as an anticoagulant in blood (19). ApoH may also modulate the function of kidney and placenta. In these organs, the membrane binding ApoH was reported to control the interaction of some other substrates with lipids directly (20, 21). The abnormality of the plasma ApoH level was shown to be associated with many diseases such as thrombocytopenia, arterial and venous thrombosis, and recurrent abortion (22, 23). In addition, it has been found that, in hyperlipidaemia, diabetes, or atherosclerosis patients, the concentration of plasma ApoH increased and the distribution of the protein among different types of lipoprotein was perturbed (24, 25). Recently, research on ApoH was given further impetus by the discovery that the lipid-associated ApoH can bind to some pathogenic antigens or proteins such as hepatitis B surface antigen (26, 27), proteins p18, p26, and gp160 of HIV (28), and anti-phospholipid antibodies (29, 30). These findings highlighted a potentially critical role of ApoH in the mechanism of infection in hepatitis B, AIDS, and systemic lupus erythematosus etc.

The interactions of ApoH with phospholipids have been considered as a basic mechanism related to its physiological and pathogenic functions. That ApoH prefers to bind to negatively charged phospholipids has been demonstrated in several laboratories (16, 31–33). Our previous work has reported that ApoH is a surface-active protein that can insert into the negatively charged membrane during its interaction with phospholipid (34). In the present paper, the characteristics of ApoH interacting with phospholipid vesicles were further examined by measuring the fluorescence data of blue shift and quenching of the protein. As a result, a model for ApoH in the membrane-bound state was set up accordingly. Our results may also help to explain how ApoH facilitates

[†] This work was supported by the National Natural Science Foundation of China.

* Correspondence should be addressed to this author at the Department of Biological Sciences & Biotechnology, Tsinghua University, Beijing 100084, People's Republic of China. Telephone: +8610-62784768; Fax: +8610-62785505; E-mail: suisf@mail.tsinghua.edu.cn.

¹ Abbreviations: ApoH, apolipoprotein H; DMPC, 1,2-dimyristoyl-sn-glycero-3-phosphocholine; DMPG, 1,2-dimyristoyl-sn-glycero-3-phosphoglycerol; CL, bovine heart cardiolipin; DPC, 1-palmitoyl-2-stearoyl-(5-doxy)-sn-glycero-3-phosphocholine; SUVs, small unilamellar vesicles.

the purging of plasmic liposomes *in vivo* (35), and the pathogenic roles of ApoH in antiphospholipid syndrome.

MATERIALS AND METHODS

Materials. 1,2-Dimyristoyl-*sn*-glycero-3-phosphoglycerol (DMPG), cardiolipin (CL, from bovine heart), 1,2-dimyristoyl-*sn*-glycero-3-phosphocholine (DMPC), and citraconic anhydride were purchased from Sigma Chemical Co. (St. Louis, MO). 1-Palmitoyl-2-stearoyl-(5-doxy)-*sn*-glycero-3-phosphocholine (DPC) was purchased from Avanti Polar Lipids (Birmingham, AL). Heparin-Sepharose CL-6B was obtained from Pharmacia (Sweden). The other chemicals used were of analytical grade made in China.

Purification of ApoH. ApoH was purified from human serum according to the method of Polz et al. (36). Briefly, 2.5 mL of perchloric acid (70%, v/v) was added to 100 mL of fresh human serum at 4 °C. After stirring for 15 min, the sample was centrifuged for 20 min under 20000g. Then the supernatant was neutralized with saturated Na₂CO₃ and dialyzed against Tris-Cl buffer (0.02 mol/L Tris-Cl, pH 8.0, 0.03 mol/L NaCl) for at least 36 h. The dialysis residue was applied to the Heparin-Sepharose CL-6B column which had been equilibrated with the same buffer. The adsorbed proteins were eluted stepwise with 0.02 mol/L Tris-Cl buffer (pH 8.0), with increasing molarity of NaCl. The fraction that was eluted in a linear NaCl gradient from 0.15 to 0.60 mol/L was dialyzed and further purified by reverse-phase HPLC. The protein sample, checked by SDS/PAGE, showed one protein band at an apparent molecular mass of 54 kDa after silver staining. Further assay by ELISA using the monoclonal antibody of ApoH confirmed that the purified protein was ApoH (37). After dialysis against bidistilled water, ApoH was freeze-dried and stored at -70 °C. The protein was redissolved in 0.05 mol/L Tris-Cl buffer (pH 7.4), containing 0.025 mol/L NaCl before use, and its concentration was determined by absorption spectroscopy ($\epsilon_{280} = 1.0 \text{ mL mg}^{-1} \text{ cm}^{-1}$) (6).

Various Treatments of ApoH. For heat inactivation, the ApoH (50 μL ; 43 μg) was incubated at 95 °C for 25 min, and then placed in ice. For reduction/alkylation study, the ApoH (100 μL ; 87 μg) was denatured in a final concentration of 4 mol/L guanidinium chloride. Reduction was performed by adding dithiothreitol to a final concentration of 40 mmol/L. After incubation for 2 h at 37 °C, the sample was alkylated with 0.1 mol/L iodoacetamide, and then dialyzed against 0.05 mol/L Tris-Cl, pH 7.4, and 0.025 mol/L NaCl overnight (31).

For Lys-modified samples, ApoH (100 μL ; 87 μg) was dissolved in water (8.0 mL), and the pH was adjusted to 8.2. Aliquots (100 μL) of citraconic anhydride were added to the magnetically stirred protein solution at 30 min intervals. A total of 800 μL of citraconic anhydride was added. Reaction was at room temperature, and a pH value of 8.2 was maintained by addition of 5 mol/L NaOH on the pH-Stat. When the addition of citraconic anhydride was complete, the reaction mixture was allowed to stir at room temperature for 2 more h at pH 8.2. The solution was then dialyzed at 4 °C against several changes of water that had been preadjusted to pH 8.5–8.8 with NH₄OH and finally freeze-dried (38).

Preparation of Phospholipid Vesicles. Small unilamellar vesicles (SUVs) were prepared as follows: lipids of the

desired composition were mixed in chloroform/methanol (3:1, v/v) and dried under a stream of nitrogen. Residual solvents were removed under high vacuum for 2–3 h. The lipid films were then resuspended and sonicated in a solution of 50 mmol/L Tris-Cl, 25 mmol/L NaCl, pH 7.4, by using a probe sonicator for approximately 2–3 min intervals to near optical clarity. The concentration of phospholipid was determined by phosphate analysis (39). The SUVs produced by this procedure were diluted to 1.0 mmol/L and used directly in all the experiments.

When lipid mixtures were used, appropriate aliquots of chloroform solution of each component were mixed and then dried together; afterward the homogeneous lipid mixture was dispersed in buffer and sonicated as usual.

Fluorescence Measurements. Fluorescence was measured with a Hitachi M850 Fluorescence Spectrophotometer using a 1-cm-square quartz fluorescence cuvette. Unless otherwise noted, the emission and excitation slit widths were set at 5 nm. Titration experiments were performed by adding aliquots of SUV (1.0 mmol/L) suspended in Tris-Cl buffer to the cuvette containing ApoH (1.0 $\mu\text{mol/L}$) dissolved in 1.6 mL of the same buffer. The resulting solution was stirred and equilibrated for at least 10 min before the spectra were acquired. The excitation wavelength for all spectra was 280 nm. Background intensity in samples without protein was subtracted, and the data of emission maximum and fluorescence intensities were determined from the corrected spectra. The temperature of the measurement was kept at 25.0 ± 1.0 °C.

For DPC quenching experiments, spin-labeled SUVs were prepared as mentioned above with the DPC concentration of 15% (molar percent). The I/I_0 values were obtained from the corrected spectra by using the fluorescence intensities at the tryptophan emission maxima of samples with and without spin-labels.

For acrylamide quenching experiment, aliquots (5 μL) of freshly prepared acrylamide (4 mol/L) stock solutions were added to the 1.6 mL protein solution. After each addition of the quencher, the emission intensity at 340 nm was measured, and the inner filter effects of acrylamide itself were corrected (40). The fluorescence quenching data were analyzed according to the modified Stern–Volmer equation for the collisional quenching (41):

$$I_0/(I_0 - I) = 1/f + 1/(fK_{SV}[Q]) \quad (1)$$

where I and I_0 are fluorescence intensities in the presence and absence of quencher, respectively, $[Q]$ is quencher concentration, and f and K_{SV} are the fractional number of accessible fluorophores and the modified collisional constant, respectively. The values of f and K_{SV} can be graphically determined by the plot of $I_0/(I_0 - I)$ versus $1/[Q]$.

RESULTS

Binding of ApoH to Phospholipid Vesicles. An ApoH molecule contains 5 tryptophan and 14 tyrosine residues. As shown in Figure 1(a), its emission maximum is centered around 345 nm, indicating that the spectrum is mainly due to the tryptophan residues and that some of the indole side chains are partially buried. Addition of negatively charged DMPG SUVs to the ApoH solution produces a significant blue shift of the ApoH fluorescence emission maximum from

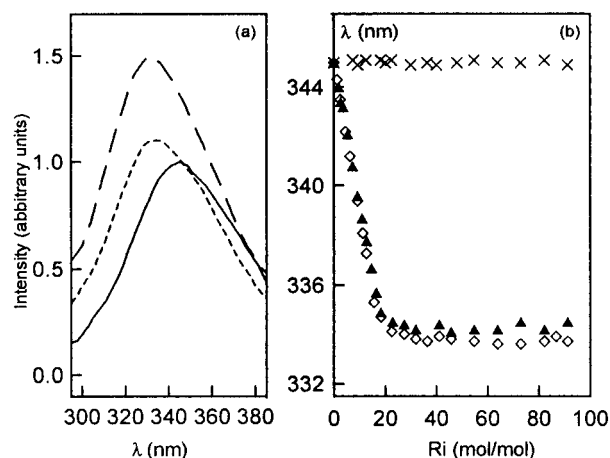


FIGURE 1: Fluorescence emission titration of ApoH with SUVs. The excitation wavelength was 280 nm. ApoH concentration was 1.0 μ M. (a) Fluorescence emission spectroscopy of ApoH. Solid line, free protein; short dashed line, binding to CL SUVs; long dashed line, binding to DMPG SUVs. (b) Droplets of SUVs (1.0 mM) were added from stock solutions to give the desired molar ratio of lipid to protein (shown as R_i) from 1.25 to 100. Crosses, DMPC; open diamonds, DMPG; closed triangles, CL. The data were averaged from duplicate measurements.

345 to 334 nm. This effect reflects the change of environment of ApoH's tryptophan residues to a less polar one and indicates an association between ApoH and phospholipids. Similar experiments have also been performed with another negatively charged phospholipid, CL [Figure 1(a)].

Figure 1(b) shows the shift of emission maximum vs the lipid to protein molar ratio (R_i). It is seen that the amplitude of the blue shift does not vary with the type of negatively charged phospholipid used (DMPG or CL). On the contrary, the addition of neutral DMPC SUVs almost did not alter the fluorescence emission maximum of ApoH even at a higher R_i value of 100. By using the technique of 90° light scattering (42), no association between ApoH and the DMPC SUVs was further demonstrated (data not shown). Therefore, it is evident that the negatively charged lipids are essential for the interaction of ApoH with phospholipid membranes.

Curves in Figure 1(b) also showed that with the addition of negatively charged SUVs, the fluorescence emission maximum of ApoH decreased linearly until a plateau value was reached. In cases where either DMPG or CL SUVs were used, the critical molar ratio (R_c) for ApoH binding, which is defined as the minimal R_i for maximal binding of protein to lipid vesicles, has the same value of about 19 ± 1 . The lipid concentrations for half-maximal blue shift for the two negatively charged SUVs are also similar to each other, implying that the two phospholipids, DMPG and CL, although differing in charge number per molecule, did not change their interaction with ApoH significantly.

Measurement of Insertion Extent of Tryptophan Residues into Phospholipid Vesicles. The observed fluorescence blue shift can be attributed to the decrease of the polarity of the tryptophan environment. To examine the insertion extent of ApoH into lipid vesicles, fluorescence quenching experiments utilizing quenchers covalently attached to the acyl chain of a phospholipid were performed. The bilayer resident quencher used was DPC, which contains an unpaired electron in its nitroxide spin-label and will act as a contact quencher of tryptophan fluorescence (43). Such a method will only be

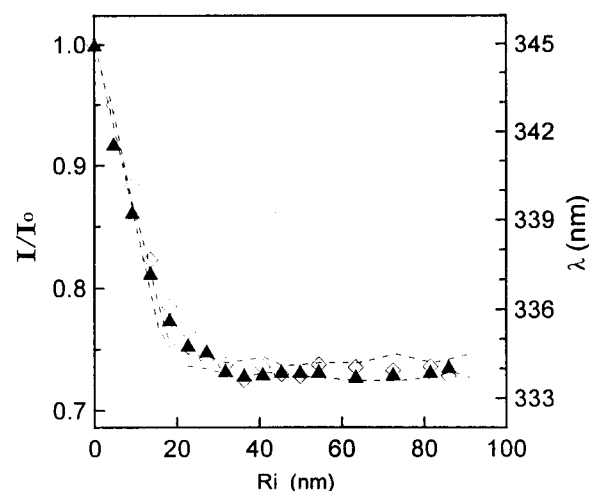


FIGURE 2: DPC quenching and wavelength shift of ApoH intrinsic fluorescence upon its binding to SUVs. Left label: fluorescence emission quenching of ApoH in the presence of DMPG (open diamonds) or CL (close triangles) SUVs containing 15% DPC. I and I_0 represent the fluorescence intensity of ApoH after binding to SUVs with or without DPC, respectively. ApoH concentration was 1.0 μ mol/L. The excitation wavelength was 280 nm. Right label: the dashed line shows the wavelength shifts of the ApoH fluorescence maximum upon SUV addition (data from Figure 1).

valid provided that at least one of the five tryptophan residues will be involved in membrane insertion. The concentration of the label was kept at 15% in all the experiments to avoid large perturbation to the lipid bilayer.

Figure 2 depicts the tryptophan fluorescence quenching of ApoH by the titration of DPC containing DMPG SUVs. The decreased fluorescence intensity indicates that at least some tryptophan residues of ApoH have inserted into the hydrophobic region of the lipid vesicles. It is also interesting to note that the DPC quenching and fluorescence emission shift curves, as compared in Figure 2, have almost the same trend upon titration of lipid vesicles, indicating simultaneous membrane binding and insertion when ApoH interacts with phospholipid vesicles.

Interaction between ApoH and Phospholipid Mixtures. The interactions of ApoH with phospholipid mixtures of DMPG and DMPC were examined in order to get more insight into the characteristics of ApoH binding to membranes. The wavelength shifts of emission maximum vs the phospholipid to protein molar ratio (R_i) are plotted in Figure 3(a). It is shown that when the PG content in the vesicle decreases from 100 to 67%, and then to 50%, the critical molar ratio (R_c) for reaching the maximum blue shift increased from 18.8 to 28.0, and then to 36.7. When vesicles containing smaller amounts of PG, i.e., 33 molar percent, were used, the curve appears as a rather smooth feature instead of a straight line before the plateau, suggesting the lower affinity for ApoH binding (see Discussion). Although in this case we cannot obtain a precise value for R_c , it can be seen approximating 60. The experimental data in Figure 3(a) can be interpreted in another way. If we replace the horizontal axis of R_i by that of the molar ratio of the negatively charged PG to protein (R_i'), we will find that all the curves in Figure 3(a) lie close together and give a similar critical molar ratio (R_c') of 18.8 ± 0.4 , strongly indicating that the fluorescence blue shift of ApoH depends only on the content of PG in the vesicles, and the PC molecules seem not to be involved in the process.

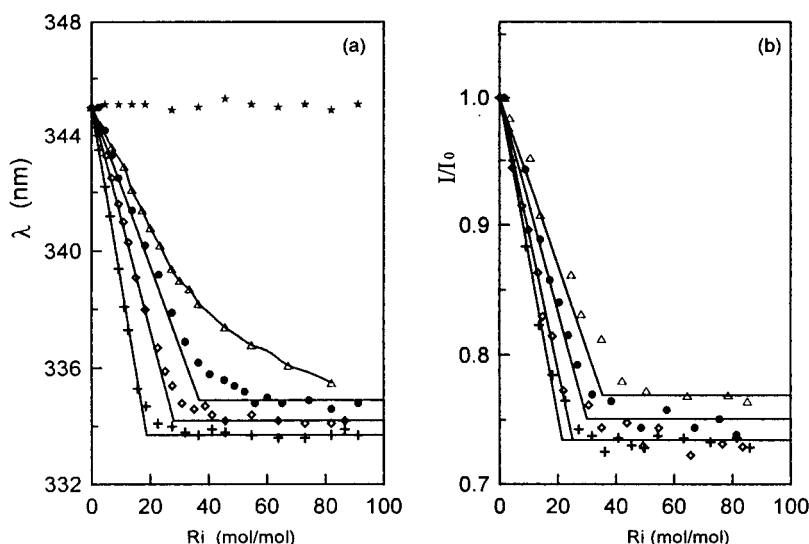


FIGURE 3: Interaction of ApoH with phospholipid mixtures. The blue shifts (a) and insertion extents (b) of ApoH upon binding to SUVs of DMPG–DMPC mixtures. The DMPG percent in the mixture vesicles is as follows: pluses, pure DMPG; open diamonds, 67%; closed circles, 50%; open triangles, 33%; stars, pure DMPC.

In contrast to the results of the blue shift, when the DPC quenching data were plotted vs the R_i [shown in Figure 3(b)], the R_c for vesicles containing 100, 67, 50, or 33% PG has a value of 21.6, 25.2, 30.0, and 35.5, respectively. It is evident that along with the decrease of PG content, the increase of R_c for quenching data is not as significant as that for the blue shift results.

Effect of Ca^{2+} on ApoH Binding to DMPG SUVs. Changing the ionic strength of the buffer will affect the electrostatic forces between the protein and the charged lipid vesicles. To see the roles of electrostatic forces in the interaction of ApoH with negatively charged vesicles, the interaction of ApoH with DMPG SUVs under Ca^{2+} environments was studied. Figure 4 depicts the fluorescence measurements on the association of ApoH to DMPG SUVs under conditions without or with 3.0 mmol/L Ca^{2+} . In the 3.0 mmol/L Ca^{2+} condition, the fluorescence blue shift of ApoH upon binding to DMPG SUVs is approximately 3.8 nm, a value about only 34% of its maximum (11.2 nm). As a control, no change in the fluorescence emission wavelength of ApoH in the absence of lipid vesicles can be observed by adding 3.0 mmol/L Ca^{2+} into the buffer (figure not shown). As to the data of DPC quenching, the value of $1 - (I/I_0)$ under conditions of 3.0 mmol/L Ca^{2+} is about 0.16, which is about 59% of its value under Ca^{2+} -free conditions (0.27). It is clearly seen that upon interaction with DMPG SUVs in the presence of Ca^{2+} , the extent of blue shift of ApoH will be influenced more significantly than that of DPC quenching.

Effect of Ionic Strength on the Detachment of ApoH from DMPG SUVs. Detachment of ApoH from DMPG SUVs by Na^+ or K^+ at concentrations of 50–1000 mmol/L was studied in order to get further insight into the forces facilitating the ApoH–membrane interaction. The results obtained are summarized in Figure 5. It is shown that the blue shift extent of ApoH greatly decreased upon the addition of these cations. At 0.5 mol/L Na^+ (K^+), the numeric value of the blue shift of ApoH remained 9% (18%) of its maxima. As a control, the fluorescence emission spectrum of ApoH in the absence of lipid vesicles cannot be affected with the experimental concentrations of Na^+ (or K^+) (figure not

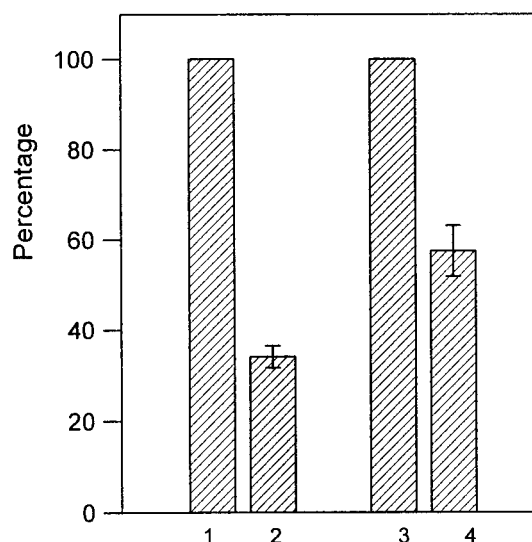


FIGURE 4: Association of ApoH with DMPG SUVs under conditions without or with 3.0 mmol/L Ca^{2+} . Bar 1 (without Ca^{2+}) and bar 2 (with 3.0 mmol/L Ca^{2+}), data of the fluorescence blue shift of ApoH upon binding to DMPG SUVs ($\Delta\lambda$). Bar 3 (without Ca^{2+}) and bar 4 (with 3.0 mmol/L Ca^{2+}), $1 - (I/I_0)$ (data from DPC quenching experiments), where I and I_0 are fluorescence intensities in the presence and absence of the quencher DPC. The data in conditions with 3.0 mmol/L Ca^{2+} (bars 2 and 4) were plotted as the percentage of those in conditions without Ca^{2+} (bars 1 and 3). The molar ratio of lipid to protein was preset at 45.

shown). Moreover, background binding to DMPC was not sensitive to any of these cations, either.

In contrast to the data of blue shift, the effect of ionic strength on the data of fluorescence quenching is not that sensitive. It is clearly seen from Figure 5 that at 0.5 mol/L Na^+ (or K^+), the insertion extent of ApoH remained approximately 50%. When the Na^+ (K^+) concentration of the buffer was raised further to 1.0 mol/L, the blue shift of ApoH reduced to nearly zero, suggesting that nearly all the tryptophan residues of ApoH were moved to a polar environment. However, even in this case, the insertion of ApoH still has nearly 20% of its maximal value, indicating that the insertion of ApoH into the DMPG membrane can

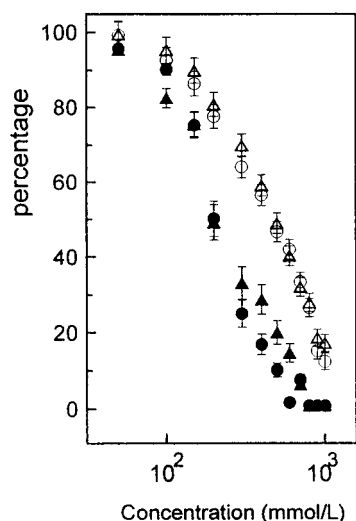


FIGURE 5: Detachment of ApoH from DMPG SUVs by Na^+ and K^+ . The blue shifts (closed symbols) and insertion extent (open symbols) of ApoH upon binding to DMPG SUVs at various concentrations of Na^+ (circles) or K^+ (triangles). The data are presented as a percentage of their values in a Na^+ (or K^+) free environment. The molar ratio of lipid to protein was preset at 45.

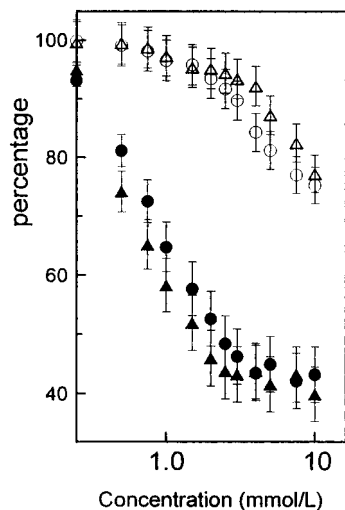


FIGURE 6: Detachment of ApoH from DMPG SUVs by Ca^{2+} and Mg^{2+} . The blue shifts (closed symbols) and insertion extent (open symbols) of ApoH upon binding to DMPG SUVs at various concentrations of Ca^{2+} (circles) or Mg^{2+} (triangles). The data are presented as a percentage of their values in a Ca^{2+} (or Mg^{2+}) free environment. The molar ratio of lipid to protein was preset at 45.

hardly be completely abolished by raising the buffer's ionic strength.

The detachment of ApoH from DMPG SUVs by various amounts of CaCl_2 or MgCl_2 was also studied in another set of experiments (Figure 6). Consistent with the results of Na^+ (K^+) (as shown in Figure 5), there is a remarkable decrease in the blue shift data of ApoH tryptophan fluorescence when increasing the CaCl_2 or MgCl_2 concentrations. As a control, the fluorescence emission spectrum of ApoH in the absence of lipid vesicles cannot be affected by the addition of Ca^{2+} or Mg^{2+} up to 20 mmol/L (figure not shown). It is clearly seen from the figure that in cases of CaCl_2 or MgCl_2 concentrations up to 10 mmol/L, the insertion extent of ApoH remains about 75% of the maximum while the blue shift extent remains only 40%. At moderately high cation concentration, e.g., around 3.0 mmol/L Ca^{2+} , the two curves of

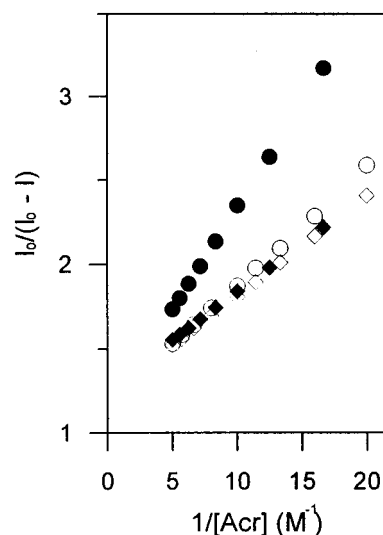


FIGURE 7: Acrylamide quenching of ApoH intrinsic fluorescence. Modified Stern–Volmer plot for the tryptophan fluorescence quenching of ApoH by acrylamide. ApoH concentration was 1.0 μM ; lipid concentration was 30 μM . The excitation wavelength was 280 nm. Closed diamonds, water-soluble ApoH in Ca^{2+} -free buffer; closed circles, membrane-bound ApoH in Ca^{2+} -free buffer; the vesicle composition is DMPG/DMPC (80:20, in molar ratio). Open diamonds, water-soluble ApoH in buffer with 3.0 mmol/L Ca^{2+} ; open circles, membrane-bound ApoH in buffer with 3.0 mmol/L Ca^{2+} ; the vesicle composition is DMPG/DMPC (80:20, in molar ratio). All the measurements were performed in triplicate, and the results were averaged.

blue shift and DPC quenching divided a lot. The extent of fluorescence quenching decreased a little (only about 10%) whereas the value of the blue shift dropped significantly (about 58%), indicating that under this condition the membrane-bound ApoH molecules adopt another conformation which is different from that under low ionic strength conditions.

To test the effect of ionic strength on the microenvironment of the tryptophan residues of the protein, acrylamide was chosen as a soluble quencher to examine the accessibility of the tryptophan residues to the aqueous solvent (as shown in Figure 7). From the data of Figure 7, it was calculated according to eq 1 that the quenching constant (K_{SV}) for ApoH in the absence of lipid is about 22.28 (mol/L) $^{-1}$. After binding to DMPG SUVs, the K_{SV} value decreases to about 9.06 (mol/L) $^{-1}$. It is known that the K_{SV} values can reflect either a decrease in exposure or a decrease in lifetime of the tryptophan residues of ApoH. However, since lifetime is often linked to intensity, the increased intensity of ApoH upon lipid binding as shown in Figure 1(a) suggests an increased lifetime upon lipid binding. Thus, the decrease in K_{SV} is likely to be due to the effective shield of ApoH tryptophan residues from the quencher. When raising the Ca^{2+} concentration of the buffer to 3.0 mmol/L, the K_{SV} value exhibits an increase from 9.06 to 16.96 (mol/L) $^{-1}$, indicating that the ApoH tryptophan residues become more accessible under this condition.

Effects of Various Treatments on ApoH Binding to Phospholipid Vesicles. To study the structure bases of ApoH that facilitate its interaction with membranes, the ApoH was first heat-inactivated for 25 min at 95 $^{\circ}\text{C}$; then the fluorescence assay was performed. The results obtained are compared with those of the natural sample (as shown in Table

Table 1: Interaction of Various Treated ApoH with DMPG SUVs: Blue Shift and Membrane Insertion Data

ApoH sample ^a	λ_{\max} (nm)		R_c^b (mol of lipid/mol of ApoH)	insertion ^c (I/I_0)
	free	membrane bound		
native	345	334	18.1 ± 1	0.73 ± 0.01
heated	348	341	17.2 ± 1	0.72 ± 0.01
reduced/alkylated	348	345	25.0 ± 2	0.78 ± 0.01
CT treated	349	346	53.0 ± 4	0.92 ± 0.04

^a ApoH samples were treated as described under Materials and Methods. ^b Data from the wavelength maximum vs R_i curves. ^c Data from DPC quenching measurements with the DMPG to ApoH molar ratio higher than the R_i values listed in the left column.

1). It is seen that the wavelength of emission maximum of the heat-treated ApoH is at 348 nm. After the addition of DMPG SUVs, it shifts to 341 nm, a value a little lower than that of the natural sample in the lipid-free condition. However, the membrane insertion ability of heat-treated ApoH does not change significantly. This result suggests that the insertion of ApoH into DMPG SUVs does not depend on its three-dimensional structure.

In another experiment, ApoH was reduced and the free -SH was alkylated to see the effect of disulfide bonds on its interaction with the membrane. After the treatment, the blue shift extent for membrane-bound ApoH was greatly reduced. However, the insertion ability of the treated ApoH changed little (data shown in Table 1). Since the structure of the Sushi domain of ApoH is maintained by the disulfide bonds, our result, on the other hand, indicates that the insertion of ApoH is not sensitive to its domain structure. Therefore, it may be a short linear sequence that determines the insertion of ApoH into membranes.

Citraconic anhydride can react with the -NH₂ group of protein under neutral pH conditions (44), so it was used to modify the Lys residues of ApoH. The results listed in Table 1 show that under such treatment, the ApoH molecules cannot associate with vesicles. Neither can it insert into the SUVs, suggesting the extremely important role of Lys residues in the course of ApoH/membrane interaction.

DISCUSSION

The interaction between ApoH and lipid membrane has been reported to be critical for the physiological roles of the protein (16, 31–33). In 1984, Wurm et al. (16) reported for the first time that the negatively charged phospholipids interacted strongly with ApoH. With a supported planar bilayer, Willems et al. (33) examined the ApoH-mediated binding of anti-cardiolipin antibodies to the lipid membranes. Our previous work has also demonstrated that ApoH can insert into phospholipid monolayers at an air/water interface (34). Nevertheless, the behavior of ApoH itself at the membrane surface is still relatively unknown until now. In the present paper, the binding and insertion abilities of ApoH to phospholipid vesicles were studied by fluorescence techniques. The first result is that when associated with the lipid membrane, the fluorescence emission maximum of ApoH will have a large blue shift of about 11 nm (as shown in Figure 1). This blue shift indicates an increase in the hydrophobicity of the ApoH's tryptophan environment, which is likely to be due to the masking of these residues by the apolar moiety of the lipid vesicles (45, 46). This

surmise was demonstrated by the experiments that the DPC quenching extent of ApoH also increased upon the addition of DMPG vesicles (shown in Figure 2). Considering the results that the changes in both blue shift and DPC quenching data have almost the same trend, it is suggested that at least some of the tryptophan residues of ApoH have inserted into the lipid bilayer upon its interaction with the lipid membrane.

Two interesting parameters are in principle accessible from the binding experiments shown in Figure 1, namely, the association constant K_a and the critical molar ratio R_c of the lipid–protein complexes. The binding of ApoH to negatively charged lipids is stoichiometric; i.e., as long as the vesicle surface is not totally covered, one observes a linear decrease in the wavelength of emission maximum (which is proportional to the amount of bound protein). This phenomenon means that the association constant (K_a) between ApoH and the negative lipid is much higher than the protein concentration (1.0 μ mol/L). Although no precise value can be given by the fluorometric titration measurement, the value of K_a is certainly $>10^6$ (mol/L)⁻¹. Our estimation is consistent with that obtained by Willems et al. (33).

The R_c value for which the plateau is reached is another useful parameter that gives the stoichiometry of complex formation (47). The data in both Figure 1(b) and Figure 2 show that the numerical value of R_c is 19 ± 1 whenever PG or CL is used, suggesting the similar characteristics of these two negatively charged lipids for ApoH interaction.

The blue shift and the quenching data for ApoH interaction with lipid mixtures of DMPG and DMPC were compared as shown in Figure 3. The blue shift of ApoH only depends on the content of DMPG [Figure 3(a)]. However, if enough PG is present, i.e., greater than 67%, the quenching extent of ApoH will have the same value as for interaction with pure DMPG SUVs [Figure 3(b)], indicating that the insertion ability of ApoH into PG-containing vesicles does not depend on the PG content in a stoichiometric way as does the blue shift. This result suggests that the negatively charged lipid DMPG does not serve as a specific binding site but rather provides a suitable microenvironment for ApoH insertion.

The bivalent Ca²⁺ can affect the intermolecular electrostatic interaction (48). Thus, it can efficiently influence the interaction between ApoH and DMPG SUVs. In the previous work of Wurm et al., they measured the detachment of ApoH from liposomes by addition of cations with centrifugation (16). In the present work, that both the blue shift and the quenching data can be reduced by addition of cations indicates the real detachment of the ApoH molecules from the lipid vesicles. An intriguing result of the present study is that the effect of cations on the blue shift is remarkably different from that on the quenching extent. From the results in Figure 4, we can see that under the condition of 3.0 mmol/L Ca²⁺, the DPC quenching extent of ApoH remains about 59% of its maximal value in the Ca²⁺-free case, whereas the blue shift data remain only about 34%. Such a phenomenon is observed in more detail in Figures 5 and 6. Under conditions of increasing ionic strength, the blue shift data of ApoH obviously decreased in buffer with 100 mmol/L Na⁺ (K⁺) or 0.5 mmol/L Ca²⁺ (Mg²⁺). However, the fluorescence quenching data exhibited a significant decrease only when buffer with much higher concentrations of cations, such as Na⁺ (K⁺) at 200 mmol/L and Ca²⁺ (Mg²⁺) at 2.5 mmol/L, was used. Since the force that facilitates the

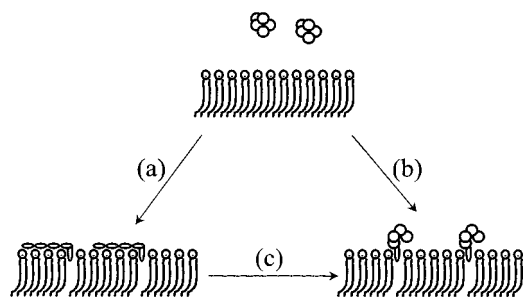


FIGURE 8: Schematic diagram of ApoH interaction with negatively charged lipid vesicles. Under conditions of low ionic strength (a), the water-soluble ApoH will bind to the negatively charged lipid vesicles with most of its tryptophan residues adsorbing on the membrane surface and a small part of them inserting into the membrane. Under conditions of 3.0 mmol/L Ca^{2+} (b), the membrane-bound ApoH will have a different conformation with its noninserted tryptophan residues mainly separated from the membrane surface, and its membrane-inserted ones still maintained their association with the membrane. When increasing the ionic strengths of buffer after the binding of ApoH to membranes (c), the conformation of membrane-bound ApoH will change from that under condition (a) to that under condition (b).

membrane insertion of a protein mainly comes from the hydrophobic interaction between the protein and the lipid, it cannot be weakened much by the addition of ions. Thus, the significant delay in the decrease of the quenching data (as shown in Figures 5 and 6) indicates a hydrophobic interaction between ApoH and the lipid membrane. It should be noted that the measured blue shift data will have a distortion due to the different fluorescence intensities of soluble and membrane-bound ApoH, both of which exist in the buffer under high ionic strength conditions. However, the estimated value of this distortion will be less than 10% of the maximum of blue shift data in all of our cases. Thus, the effect of this distortion is small. Moreover, it is interesting to note that the data concerning the effect of Ca^{2+} on the insertion of ApoH into lipid vesicles fit well with our previous work of lipid monolayer study (34), both suggesting that the membrane insertion of ApoH cannot be affected much by increasing the ionic strength of the buffer.

ApoH exhibits both water-soluble and membrane-bound states. Combining all the data mentioned above, we could determine the conformation of protein in the membrane-bound state. Under conditions of low ionic strength, most of the tryptophan residues of ApoH adsorbed on the membrane surface with a small part of them being involved in membrane insertion. When the ionic strength of the buffer increased, the loosely surface-located tryptophan residues of ApoH will be gradually detached from the vesicles, while the membrane-inserted ones still maintained their association with the membrane. During this process, the blue shift data of ApoH are remarkably reduced whereas the DPC quenching data have a delayed response. Our opinion that ApoH is capable of existing in two different conformations when membrane-bound is depicted in Figure 8 in a schematic way.

The isoelectric point of ApoH is 5–7 (51), so the protein is negatively charged under pH 7.4 conditions. It is unexpected that a negatively charged protein preferentially inserts into membranes of negatively charged lipids. To reveal the structure base for ApoH insertion, we altered the structure of ApoH by various treatments and studied the influence of these treatments on ApoH–membrane interaction. The results

collected in Table 1 showed that the emission maximum of ApoH in the absence of vesicles undergoes a red shift under any of these treatments, e.g., heated, reduced/alkylated, or Lys-modified. After binding to DMPG SUVs, only a small blue shift was observed, suggesting the weak influence of vesicle on the conformation of the protein. From the quenching data, it is seen that the insertion ability of ApoH is independent of its three-dimensional or domain structure, but is closely related to its Lys residues. These results suggest that a heat-stable and disulfide bond-independent motif, which may be a sequential region rich in positively charged Lys residues, facilitates the insertion of ApoH into the negatively charged vesicles. Our findings are consistent with that of Kertesz et al., who recently showed that a conserved sequence ($\text{C}^{281}\text{KNKEKK}\text{C}^{288}$) rich in basic residues is important for the interaction of ApoH with phospholipid (31).

It is reported that in vivo ApoH is one of the major proteins appearing in the very rapidly cleared large liposomes that contain phosphatidylcholine, cholesterol, and negatively charged phospholipids (35). Since these negatively charged phospholipids are normally found exclusively in the interior of cells but become expressed when cells undergo apoptosis or programmed cell death, they are believed to be markers of cell senescence (52). The immune clearance rate of these liposomes from the circulation is associated with the amount of adsorbed ApoH and negatively charged lipids (35, 53), but the reason is unknown. Our results here give direct proof that ApoH can specifically bind and actually insert into these negatively charged liposomes. Thus, it can perform its biological function as a “Cleaner” to purge the plasmic liposomes coming from senescent cells and foreign particles.

ApoH has also been described to serve as a cofactor for the binding of some anti-phospholipid antibodies to membranes containing negative phospholipids (for review, see 54). Such anti-phospholipid antibodies that appeared in high titers in some autoimmune diseases, and anti-phospholipid syndrome etc. were considered to be pathogenic in vivo. That these antibodies recognized in vivo neither ApoH nor the lipid alone has been established (54, 55). Therefore, it is supposed that the antibodies may actually bind to the new determinants of ApoH, which were specifically exposed during the ApoH–membrane interactions. This idea can be well supported by our findings here that ApoH will adopt a specific conformation when bound to the negatively charged membranes. Also the idea will be supported that the anti-phospholipid antibodies cannot bind to complexes between ApoH and heparin, although the conformation of ApoH in this case may be changed, too (30, 56). Nevertheless, it is worthy of noting that although the findings about the membrane insertion and conformational changes of ApoH give critical clues to the protein function, the exact physiological and pathogenic roles of ApoH, for example, the exact role of ApoH in the formation of the anti-phospholipid–phospholipid complex, are still relatively unknown. The biological function of ApoH in vivo warrants further investigation.

REFERENCES

- Schultze, H. E., Heide, K., and Haupt, H. (1961) *Naturwissenschaften* 23, 719.
- Lozier, J., Takahashi, N., and Putnam, F. W. (1984) *Proc. Natl. Acad. Sci. U.S.A.* 81, 3640–3644.

3. Kristensen, T., Schousboe, I., Boel, E., Mulvihill, E. M., Hansen, R. R., Moller, K. B., Moller, N. P. H., and Sottrup-Jensen, L. (1991) *FEBS Lett.* 289, 483–486.
4. Mehdi, H., Nunn, M., Steel, D. M., Whitehead, A. S., Perez, M., Walker, L., and Peeples, M. E. (1991) *Gene* 108, 293–298.
5. Steinkasserer, A., Estaller, C., Weiss, E. H., Sim, R. B., and Day, A. J. (1991) *Biochem. J.* 277, 387–391.
6. Kato, H., and Enjyoji, K. (1991) *Biochemistry* 30, 11687–11694.
7. Bendixen, E., Halkier, T., Magnusson, S., Sottrup-Jensen, L., and Kristensen, T. (1992) *Biochemistry* 31, 3611–3617.
8. Nonaka, M., Matsuda, Y., Shiroishi, T., Moriwaki, K., Nonaka, M., and Natsuume-Sakai, S. (1992) *Genomics* 13, 1082–1087.
9. Aoyama, Y., Chan, Y. L., and Wool, I. G. (1989) *Nucleic Acids Res.* 17, 6401.
10. Ichinose, A., Bottenus, R. E., and Davie, E. W. (1990) *J. Biol. Chem.* 265, 13411–13414.
11. Norman, D. G., Barlow, P. N., Baron, M., Day, A. J., Sim, R. B., and Campbell, I. D. (1991) *J. Mol. Biol.* 219, 717–725.
12. Barlow, P. N., Norman, D. G., Steinkasserer, A., Horne, T. B., Pearce, J., Driscoll, P. C., Sim, R. B., and Campbell, I. D. (1992) *Biochemistry* 31, 3626–3634.
13. Barlow, P. N., Steinkasserer, A., Norman, D. G., Kieffer, B., Wiles, A. P., Sim, R. B., and Campbell, I. D. (1993) *J. Mol. Biol.* 232, 268–284.
14. Kroll, J., Larsen, J. K., Loft, H., Ezban, M., Wallevik, K., and Faber, M. (1976) *Biochim. Biophys. Acta* 434, 490–501.
15. Schousboe, I., and Rasmussen, M. S. (1988) *Int. J. Biochem.* 20, 787–792.
16. Wurm, H. (1984) *Int. J. Biochem.* 16, 511–515.
17. Puurunen, M., Jokiranta, S., Vaarala, O., and Meri, S. (1995) *Scand. J. Immunol.* 42, 547–550.
18. Wurm, H., Beubler, E., Polz, E., Holasek, A., and Kostner, G. (1982) *Metabolism* 31, 484–486.
19. Brighton, T. A., Hogg, B. J., Dai, Y. P., Murray, B. H., Chong, B. H., and Chesterman, C. N. (1996) *Br. J. Haematol.* 93, 185–194.
20. Klaerke, D. A., Rojkaer, R., Christensen, L., and Schousboe, I. (1997) *Biochim. Biophys. Acta* 1339, 203–216.
21. Chamley, L. W., Allen, J. L., and Johnson, P. M. (1997) *Placenta* 18, 403–410.
22. Shiozaki, A., Niiya, K., Higuchi, F., Tashiro, S., Arai, T., Izumi, R., and Sakuragawa, N. (1994) *Thromb. Res.* 76, 199–210.
23. Blank, M., Faden, D., Tincani, A., Kopolovic, J., Goldberg, I., Gilburd, B., Allegri, F., Balestrieri, G., Valesini, G., and Shoenfeld, Y. (1994) *J. Autoimmun.* 7, 441–455.
24. McNally, T., Crook, M., Mackie, I. J., Isenberg, D. A., and Machin, S. J. (1994) *Br. J. Haematol.* 88, 424–426.
25. Cassader, M., Ruiiu, G., Gambino, R., Veglia, F., and Pagano, G. (1997) *Metab., Clin. Exp.* 46, 522–525.
26. Mehdi, H., Kaplan, M. J., Anlar, F. Y., Yang, X., Bayer, R., Sutherland, K., and Peeples, M. E. (1994) *J. Virol.* 68, 2415–2424.
27. Neurath, A. R., and Strick, N. (1994) *Virology* 204, 475–477.
28. Stefan, E., Rucheton, M., Graafland, I., Moynier, M., Sompey-rac, C., Bahraoui, E. M., and Veas, F. (1997) *AIDS Res. Hum. Retroviruses* 13, 97–104.
29. Galli, M., Comfurius, P., Maassen, C., Hemker, H. C., de Baets, M. H., van Breda Vriesman, P. J., Barbui, T., Zwaal, R. F., and Bevers, E. M. (1990) *Lancet* 335, 1544–1547.
30. McNeil, H. P., Simpson, R. J., Chesterman, C. N., and Krilis, S. A. (1990) *Proc. Natl. Acad. Sci. U.S.A.* 87, 4120–4125.
31. Kertesz, Z., Yu, B. B., Steinkasserer, A., Haupt, H., Benham, A., and Sim, R. B. (1995) *Biochem. J.* 310, 315–321.
32. Hagihara, Y., Goto, Y., Kato, H., and Yoshimura, T. (1995) *J. Biochem.* 118, 129–136.
33. Willems, G. M., Janssen, M. P., Pelsers, M. M. A., Comfurius, P., Galli, M., Zwaal, R. F. A., and Bevers, E. M. (1996) *Biochemistry* 35, 13833–13842.
34. Wang, S. X., Cai, G. P., and Sui, S. F. (1998) *Biochem. J.* 335, 225–232.
35. Chonn, A., Semple, S. C., and Cullis, P. R. (1995) *J. Biol. Chem.* 270, 25845–25849.
36. Polz, E., Wurm, H., and Kostner, G. M. (1980) *Int. J. Biochem.* 11, 265–270.
37. Cai, G., Satoh, T., and Hoshi, H. (1995) *Biochim. Biophys. Acta* 1269, 13–18.
38. Habeeb, A. F. S. A., and Atassi, M. Z. (1970) *Biochemistry* 9, 4939–4944.
39. Ames, B. N. (1966) *Methods Enzymol.* 8, 115–118.
40. Calhoun, D. B., Vanderkooi, J. M., and Englander, S. W. (1983) *Biochemistry* 22, 1533–1539.
41. Lehrer, S. S. (1971) *Biochemistry* 10, 3254–3262.
42. Nelsestuen, G. L., and Lim, T. K. (1977) *Biochemistry* 16, 4164–4171.
43. Chattopadhyay, A., and London, E. (1987) *Biochemistry* 26, 39–45.
44. Lundblad, R. L. (1995) in *Techniques in Protein Modification*, pp 129–162, CRC Press, Boca Raton, FL.
45. Jain, M. K., Rogers, J., Simpson, L., and Gierasch, L. M. (1984) *Biochim. Biophys. Acta* 816, 153–162.
46. Le Doan, T., El Hajji, M., Rebuffat, S., Ragesvari, M. R., and Bodo, B. (1986) *Biochim. Biophys. Acta* 858, 1–5.
47. Dufourcq, J., and Faucon, J.-F. (1978) *Biochemistry* 17, 1170–1176.
48. MacDonald, R. C., Simon, S. A., and Baer, E. (1976) *Biochemistry* 15, 885–891.
49. Hunt, J. E., Simpson, R. J., and Krilis, S. A. (1993) *Proc. Natl. Acad. Sci. U.S.A.* 90, 2141–2145.
50. Hunt, J., and Krilis, S. (1994) *J. Immunol.* 152, 653–659.
51. Richer, A., and Cleve, H. (1988) *Electrophoresis* 9, 317–322.
52. Connor, J., Pak, C. C., and Schroit, A. J. (1994) *J. Biol. Chem.* 269, 2399–2404.
53. Balasubramanian, K., Chandra, J., and Schroit, A. J. (1997) *J. Biol. Chem.* 272, 31113–31117.
54. Cines, D. B., and McCrae, K. R. (1995) *J. Clin. Immunol.* 15, 86S–100S.
55. Arvieux, J., Roussel, B., Jacob, M. C., and Colomb, M. G. (1991) *J. Immunol. Methods* 143, 223–229.
56. Wagenknecht, D. R., and McIntyre, J. A. (1992) *Thromb. Res.* 68, 495–500.

BI990084S